Homogeneous vs heterogeneous subduction zone models: Coseismic and postseismic deformation

T. Masterlark[1], C. DeMets, and H.F. Wang

University of Wisconsin-Madison, Madison, Wisconsin

O. Sánchez

Instituto de Geofísica, UNAM, México D. F., México

J. Stock

California Institute of Technology, Pasadena, California

Abstract. A finite-element model (FEM) incorporating geologic properties characteristic of a subduction zone is compared with FEMs approximating homogeneous elastic half-spaces (HEHS)s to investigate the effect of heterogeneity on coseismic and postseismic deformation predictions for the 1995 Colima-Jalisco M_w=8.0 earthquake. The FEMs are used to compute a coefficient matrix relating displacements at observation points due to unit dislocations of contact-node pairs on the fault surface. The Green's function responses are used to solve the inverse problem of estimating dislocation distributions from coseismic GPS displacements. Predictions from the FEM with heterogeneous material properties, loaded with either of the HEHS dislocation distributions, significantly overestimate coseismic displacements. Postseismic deformation predictions are also sensitive to the coseismic dislocation distribution, which drives poroelastic and viscoelastic relaxation. FEM-generated Green's functions, which allow for spatial variations in material properties, are thus preferable to those that assume a simple HEHS because the latter leads to dislocation distributions unsuitable for predicting the postseismic response.

Introduction

Three-dimensional finite-element models (FEM)s are capable of simulating tectonic deformation during all phases of the seismic cycle because they allow for heterogeneous material property distributions, complicated boundary condition and loading specifications, and contact surface interactions. These models require a dislocation source to drive the coseismic response and the subsequent poroelastic and viscoelastic relaxation.

Analytical solutions to compute Green's functions for displacement due to a dislocation are readily available [*Okada*, 1992]. These solutions, which include homogeneous elastic half-space (HEHS) assumptions, are often used in inverse methods to solve for dislocation distributions based on observed coseismic deformation. Alternative methods for generating displacement Green's functions, allowing for heterogeneous material property distributions, require half-space boundary conditions [*Du et al.*, 1997; *Savage*, 1998].

Using the 1995 Colima-Jalisco earthquake as an example, we compute FEM-generated Green's functions for both drained and undrained HEHS models and for a system with spatially varying material properties characteristic of a subduction zone. Dislocation distributions are estimated from inversion of GPS displacements. We then estimate coseismic and postseismic deformation prediction errors introduced by homogeneous material property assumptions and the sensitivity to drained versus undrained conditions.

The 9 October 1995 (M_w=8.0) Colima-Jalisco earthquake, which ruptured the Rivera-North American plate subduction interface (Figure 1), was the first significant rupture of the Middle America trench northwest of the Manzanillo trough since the 3 June 1932 (M_w=8.2) and 18 June 1932 (M_w=7.8) earthquakes [*Singh et al.*, 1985]. Inversions, with HEHS model assumptions, of 3-D coseismic displacements from 11 nearby GPS sites suggest that the seismic moment release was concentrated in two regions, one near the northwest edge of the Manzanillo trough and the other 80-120 km farther northwest [*Melbourne et al.*, 1997; *Hutton et al.*, 2001], in accord with seismologic results [*Mendoza and Hartzell*, 1999].

Assumptions and Techniques: FEM

FEMs in this study were constructed with *ABAQUS* [*HKS, Inc.*, 2000], a commercial finite-element code that allows for poroelastic and viscoelastic material properties and contact surface interactions. A three-dimensional FEM was designed to simulate the subduction zone along the Middle America trench (Figure 2). The 28-km-thick continental crust [*Pardo and Suárez*, 1995] of the North American plate consists of a 16-km-thick poroelastic upper crust overlying a 12-km-thick linear viscoelastic lower crust. The oceanic crust of the Rivera plate is assumed to be 6 km thick. Poroelastic effects are neglected in the oceanic crust because they are poorly constrained by the lack of offshore GPS displacements. The upper mantle extends from the base of the crust in both plates to a depth of about 200 km and is treated as an elastic material. Zero displacement is specified along the lateral boundaries and base of the problem domain. The top

---

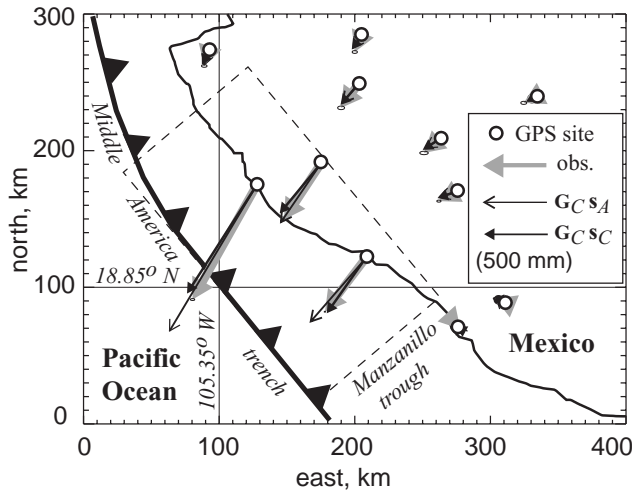[1]Now with Raytheon ITSS Corporation, USGS/EROS Data Center, Sioux Falls, SD.

Figure 1. Coseismic horizontal GPS displacements for the 1995 (M_w=8.0) Colima-Jalisco earthquake. The rupture surface intersects the Middle America trench and dips to the northeast. The dashed rectangle is the surface projection of the rupture. Predictions from $\mathbf{G}_C$ loaded with $\mathbf{s}_A$ significantly overestimate the deformation magnitudes of the coastal sites. $\mathbf{G}_C\mathbf{s}_A$ and $\mathbf{G}_C\mathbf{s}_C$ are described in the text.

of the problem domain is an elastic free surface. The boundaries of the poroelastic upper crust are no-flow surfaces.

Parameters chosen are as follows: poroelastic and drained elastic properties for Westerly Granite [*Wang*, 2000] are used for the poroelastic upper crust and viscoelastic lower crust
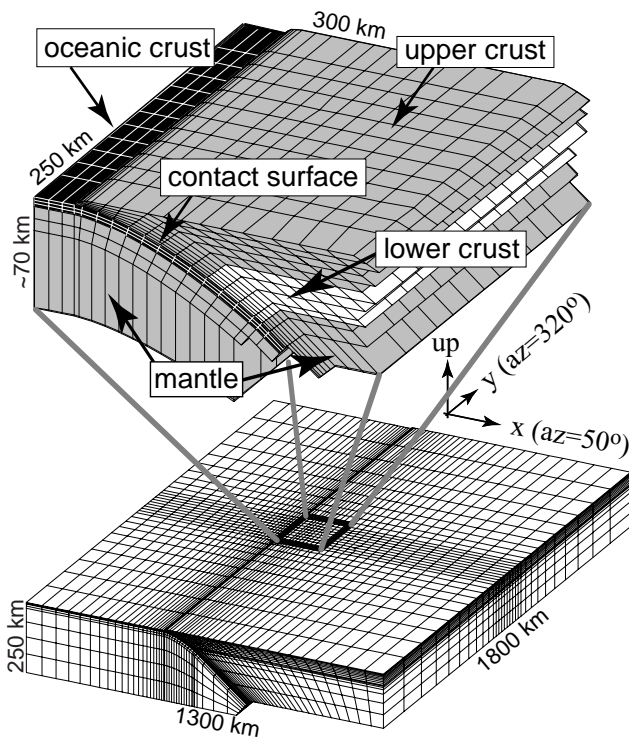

Figure 2. FEM configuration, FEM_C. The problem domain is tessellated into 24,750 three-dimensional elements. The expanded ~70 km-thick portion of the near-field region displays the heterogeneous material property distribution and subduction zone geometry.

Table 1. Weighted Least-Squares Misfit.

Model	Configuration	χ^2
Hutton et al. [2000]	*homogeneous, drained*	166
$\mathbf{G}_A\ \mathbf{s}_A$	*homogeneous, drained*	171
$\mathbf{G}_B\ \mathbf{s}_B$	*homogeneous, undrained*	171
$\mathbf{G}_C\ \mathbf{s}_C$	*heterogeneous, undrained*	164
$\mathbf{G}_C\ \mathbf{s}_A$	*inconsistent load*	9000
$\mathbf{G}_C\ \mathbf{s}_B$	*inconsistent load*	8000

layers respectively. The bulk hydraulic diffusivity of the upper crust is $10^{-2}\text{m}^2\cdot\text{s}^{-1}$ [*Nur and Walder*, 1992; *Masterlark*, 2000] and the lower crust viscosity is $5\times10^{18}\text{Pa}\cdot\text{s}$ [*Masterlark*, 2000]. We use typical elastic properties for oceanic crust and mantle rock [*Turcotte and Schubert*, 1982].

The fault is a convex, deformable contact surface divided into subfaults that measure 20×10 km along-strike and down-dip respectively [*Hutton et al.*, 2001]. Contact-node pairs are located at the center of each patch and along the top edge of the fault patches that intersect the free surface. The two lithospheric plates are welded together along the down-dip and along-strike extensions of the seismogenic portion of the interface. Initial stress and fluid-pressure conditions are geostatic.

The three mechanical systems considered are FEM_A: drained HEHS, FEM_B: undrained HEHS, and FEM_C: a heterogeneous material property distribution and poroelastic upper crust. For the two HEHS models, upper crust material properties are specified throughout the system. Drained conditions imply fluid-pressure does not change, a condition assumed in the vast majority of studies of active faults including previous solutions for dislocation distributions of the 1995 Colima-Jalsco earthquake [*Melbourne et al.*, 1997; *Mendoza and Hartzell*, 1999; *Hutton et al.*, 2001]. Undrained conditions exist in the poroelastic upper crust immediately after a sudden dislocation because stress is transferred throughout the system much faster than fluids can flow [*Wang*, 2000].

The forward solution for displacements due to a dislocation distribution in an elastic material is a linear system of equations $\mathbf{G}\ \mathbf{s} = \mathbf{d}$ for an *a priori* fault geometry, where $\mathbf{G}$ is the matrix of displacement Green's functions, $\mathbf{s}$ is a vector of dislocations for contact-node pairs, and $\mathbf{d}$ is a vector of displacements. Symbolically, the coefficient $\mathbf{G}_{ij}$ is a displacement component at location j due to a unit dislocation of contact-node pair i. For the case of the 1995 Colima-Jalisco earthquake, we consider reverse-slip only [*Melbourne et al.*, 1997; *Hutton et al.*, 2001].

We inverted the 11 measured 3-D coseismic displacements from *Hutton et al.* [2001] to obtain the mixed-determined solution for $\mathbf{s}$ using damped least-squares methods. A weighting matrix is applied to the data vector to account for uncertainties. Models FEM_A, FEM_B, and FEM_C generate $\mathbf{G}_A$, $\mathbf{G}_B$, and $\mathbf{G}_C$, which are used to obtain dislocation distributions $\mathbf{s}_A$, $\mathbf{s}_B$, and $\mathbf{s}_C$ respectively. The weighted least-squares misfits, χ^2, from the three models are similar to those determined by *Hutton et al.* [2001] (Table 1).

Dislocation magnitudes determined for an undrained material will be lower than for a drained material because undrained material properties are stiffer than their drained counterparts. The heterogeneous model (FEM_C), which simulates slip along the deformable interface between oceanic and continental crust, is the stiffest of the three cases we con-
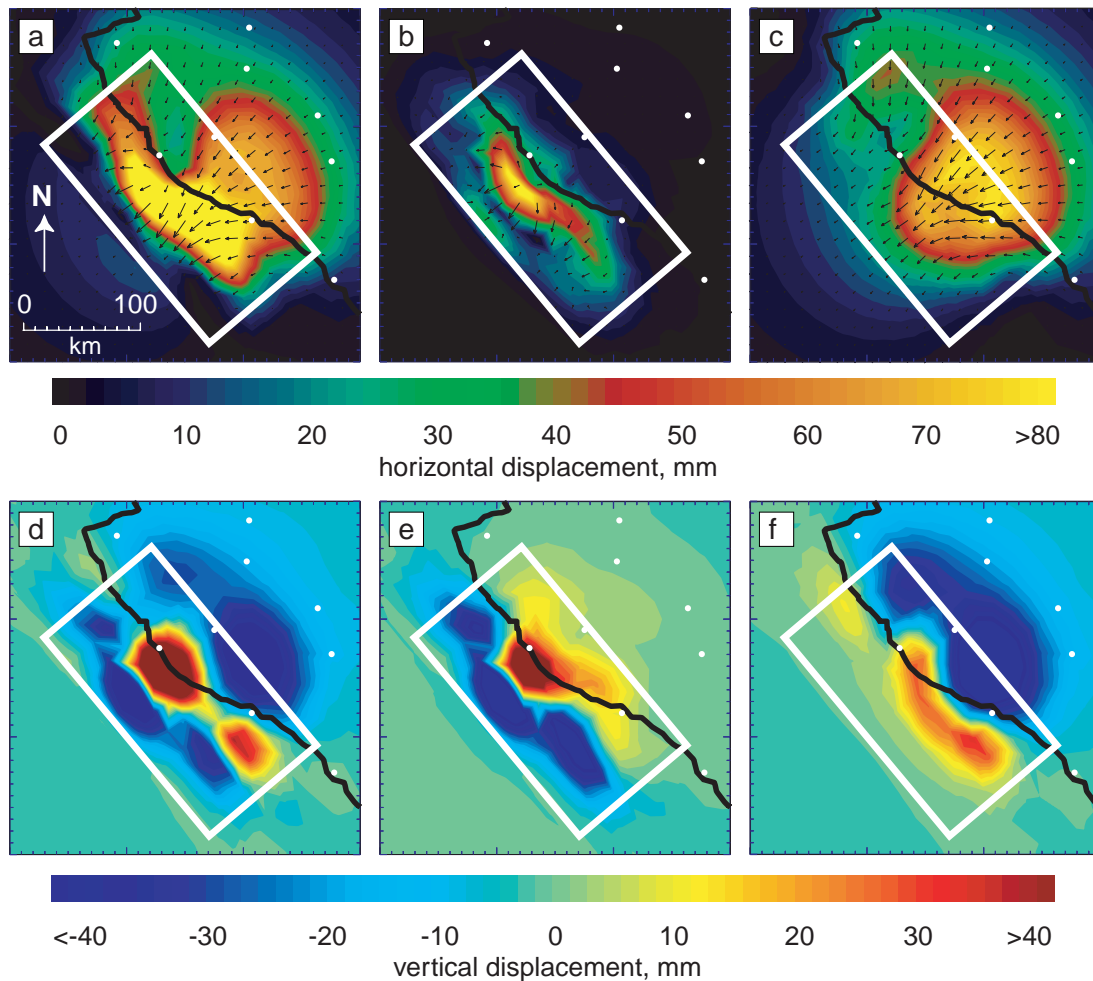
Figure 3. Net horizontal (a-c) and vertical (d-f) postseismic displacements five years after the 1995 earthquake predicted by FEM_C for dislocation source $\mathbf{s}_C$. Surface projection of the fault (rectangle), GPS sites (dots), and coastline are shown for reference. Vectors in (a-c) are predicted displacements. (a) and (d) Combined poroelastic and viscoelastic relaxation. (b) and (e) Poroelastic relaxation. (c) and (f) Viscoelastic relaxation. Poroelastic deformation occurs mostly offshore. Deformation from viscoelastic relaxation extends significantly further inland.

sidered due to the undrained upper crust and oceanic crust and mantle properties. Predicted seismic moments are 6.9, 6.7, and 6.5×10^{20}N·m for $\mathbf{s}_A$, $\mathbf{s}_B$, and $\mathbf{s}_C$ respectively, near the mid-point of seismologic estimates.

Results

Coseismic Predictions

There are substantial differences between coseismic predictions from FEM_C, loaded with $\mathbf{s}_C$ (the appropriate load) and either $\mathbf{s}_A$ (Figure 1) or $\mathbf{s}_B$. Predictions from both $\mathbf{s}_A$ and $\mathbf{s}_B$ but using the coefficient matrix $\mathbf{G}_C$ overestimate displacements for the coastal GPS sites by as much as 250 mm, much more than the $\sim$6 mm displacement uncertainty. Weighted least-squares misfits from these two models are more than an order of magnitude larger than for displacements predicted by $\mathbf{s}_C$ and using $\mathbf{G}_C$ (Table 1). These differences are expected based on the inconsistency between the model used to obtain the dislocation distribution and the one used to predict the displacements. These differences are also found in previous studies that used numerical methods to estimate the importance of heterogeneity on coseismic

deformation predictions [*Eberhart-Phillips and Stuart*, 1992; *Wald and Graves*, 2001].

Postseismic Predictions

The coseismic response of the model to the dislocation load represents the initial conditions for the postseismic model. Fluid-pressure in the upper crust and shear stress in the lower crust, initiated by fault slip, drive poroelastic and viscoelastic relaxation. For a time step of 5 years after the earthquake, which allows for both poroelastic and viscoelastic relaxation contributions, FEM_C loaded with $\mathbf{s}_C$ predicts a horizontal displacement pattern of convergence toward the rupture and subsidence nearly everywhere onshore (Figure 3).

Differences between postseismic horizontal displacements predicted by FEM_C, loaded with $\mathbf{s}_C$ versus $\mathbf{s}_A$, can be more than an order of magnitude greater than typical uncertainties ($\sim$6 mm) in GPS displacements. Although differences in vertical predictions are similar in magnitude, the uncertainties in vertical GPS displacements are much higher ($\sim$15 mm). The root-mean-squared-error in postseismic predictions, with respect to FEM_C loaded with $\mathbf{s}_C$, for loca-

tions corresponding to the 11 GPS sites is 6 mm and 5 mm for FEM_C loaded with $\mathbf{s}_A$ and $\mathbf{s}_B$ respectively. The comparisons thus far represent the sensitivity to heterogeneous material properties.

The two homogeneous FEMs and their dislocation distributions are used to estimate sensitivity to poroelastic effects. The prediction difference between the initially undrained HEHS (FEM_B), loaded with $\mathbf{s}_B$ versus $\mathbf{s}_A$, approximates the error introduced by using a dislocation distribution, determined for a drained condition assumption, in a model that includes an undrained condition assumption. In this case, the maximum differences in the postseismic horizontal and vertical displacements are 18 mm and 13 mm respectively. The horizontal differences exceed the uncertainties in the GPS displacements. The dislocation distributions derived from HEHS models that assume drained conditions should thus not be used to drive models of postseismic poroelastic deformation [*Peltzer et al.*, 1998; *Masterlark*, 2000].

Conclusions

HEHS assumptions are unnecessary, except for simple first-order approximations, because FEM-generated Green's functions allow for realistic heterogeneous material property distributions, complicated boundary condition and loading specifications, and contact surface interactions. For the 1995 Colima-Jalisco M_w=8.0 earthquake, the errors introduced in both coseismic and postseismic deformation predictions by including HEHS assumptions exceed by an order of magnitude the estimated uncertainties in the GPS displacements.

References

Du., Y., P. Segall, and H. Gao, Quasi-Static Dislocations in Three-Dimensional Inhomogeneous Media, *Geophys. Res. Lett., 24*, 2347-2350, 1997.

Eberhart-Phillips, D., and W.D. Stuart, Material Heterogeneity Simplifies the Picture: Loma Prieta, *Bull. Seism. Soc., 82*, 1964-1968, 1992.

Hutton, W., C. DeMets, O. Sanchez, G. Suarez, and J. Stock, Slip Kinematics and Dynamics During and After the 9 October 1995 Mw=8.0 Colima-Jalisco Earthquake, Mexico, from GPS Geodetic Constraints, *Geophys. Jour. Int.*, accepted for publication, 2001.

Masterlark, T.L., Regional Fault Mechanics Following the 1992 Landers Earthquake, Ph.D. Thesis, 83 pp., University of Wisconsin-Madison, Madison, Wisconsin, 2000.

Melbourne, T., I. Carmichael, C. DeMets, K. Hudnut, O. Sanchez, J. Stock, G. Suarez, and F. Webb, The Geodetic Signature of the M8.0 Oct. 9, 1995, Jalisco Subduction Earthquake, *Geophys. Res. Lett., 24*, 715-718, 1997.

Mendoza, C., and S. Hartzell, Fault-Slip Distribution of the 1995 Colima-Jalisco, Mexico, Earthquake, *Bull. Seism. Soc., 89*, 1338-1344, 1999.

Nur, A. and J. Walder, Hydraulic Pulses in the Earth's Crust, in *Fault Mechanics and Transport Properties of Rocks*, Edited by B. Evans and T.F. Wong, pp. 461-473, Academic Press, London, 1992.

Okada, Y., Internal Deformation due to Shear and Tensile Faults in a Half-Space, *Bull. Seism. Soc., 82*, 1018-1040, 1992.

Pardo, M., and Suárez, Shape of the Subducted Rivera Plate in Southern Mexico: Seismic and Tectonic Implications, *J. Geophys. Res., 100*, 12357-12373, 1995.

Peltzer, G., P. Rosen, F. Rogez, and K. Hudnut, Postseismic Rebound Along the Landers 1992 Earthquake Surface Rupture, *J. Geophys. Res., 103*, 30131-30145, 1998.

Savage, J.C., Displacement field for an edge dislocation in a layered half-space, *J. Geophys. Res., 103*, 2439-2446, 1998.

Singh, S. K., L. Ponce, and S.P. Nishenko, The Great Jalisco, Mexico, Earthquakes of 1932: Subduction of the Rivera Plate, *Bull. Seismol. Soc. Am., 75*, 1301-1313, 1985.

Turcotte, D.L., and G.J. Schubert, *Geodynamics*, 450 pp., John Wiley & Sons, New York, 1982.

Wald, D.J., and R.W. Graves, Resolution Analysis of Finite Fault Source Inversion using One- and Three-Dimensional Green's Functions 2. Combining Seismic and Geodetic Data, *J. Geophys. Res., 106*, 8767-8788, 2001.

Wang, H.F., *Theory of Linear Poroelasticity: with Applications to Geomechanics and Hydrogeology*, 287 pp., Princeton University Press, Princeton, New Jersey, 2000.

T. Masterlark, C. DeMets, and H.F. Wang, Dept. of Geology & Geophysics, UW-Madison, Madison, WI 53706. (e-mail: Masterlark@usgs.gov;chuck@geology.wisc.edu; wang@geology.wisc.edu)

J. Stock, Seismological Laboratory, California Institute of Technology, Pasadena, CA 91125 (e-mail: jstock@gps.caltech.edu)

O. Sánchez, Instituto de Geofísica, UNAM, México D. F., México (e-mail: osvaldo@ollin.igeofcu.unam.mx)